sustainability

MDPI

Article

Optimal Design of a Hybrid Solar PV/BG-Powered Heterogeneous Network

Md. Sanwar Hossain [1,*], Khondoker Ziaul Islam [2,*], Abdullah G. Alharbi [3], Md Shafiullah [4], Md. Rabiul Islam [5] and Afef Fekih [6]

[1] Department of Electrical and Electronic Engineering, Bangladesh University of Business and Technology, Dhaka 1216, Bangladesh
[2] Discipline of Information Technology, Murdoch University, Murdoch, WA 6150, Australia
[3] Department of Electrical Engineering, Faculty of Engineering, Jouf University, Sakaka 42421, Saudi Arabia; a.g.alharbi@ieee.org
[4] Interdisciplinary Research Center for Renewable Energy and Power Systems, King Fahd University of Petroleum & Minerals, Dhahran 31261, Saudi Arabia; shafiullah@kfupm.edu.sa
[5] School of Electrical, Computer and Telecommunications Engineering, University of Wollongong, Sydney, NSW 2522, Australia; mrislam@uow.edu.au
[6] Department of Electrical and Computer Engineering, University of Louisiana at Lafayette, Lafayette, LA 70504, USA; afef.fekih@louisiana.edu
* Correspondence: sanwar@bubt.edu.bd (M.S.H.); zia.islam@murdoch.edu.au (K.Z.I.)

Abstract: The increased penetration of renewable energy sources (RESs) along with the rise in demand for wireless communication had led to the need to deploy cellular base stations powered by locally accessible RESs. Moreover, networks powered by renewable energy sources have the ability to reduce the costs of generating electricity, as well as greenhouse gas emissions, thus maintaining the quality of service (QoS). This paper examines the techno-economic feasibility of developing grid-tied solar photovoltaic (PV)/biomass generator (BG)-powered heterogeneous networks in Bangladesh, taking into account the dynamic characteristics of RESs and traffic. To guarantee QoS, each macro and micro-base station is supplied through a hybrid solar PV/BG coupled with enough energy storage devices. In contrast, pico and femto BSs are powered through standalone solar PV units due to their smaller power rating. A hybrid optimization model for electric renewables (HOMER)-based optimization algorithm is considered to determine the optimum system architecture, economic and environmental analysis. MATLAB-based Monte-Carlo simulations are used to assess the system's throughput and energy efficiency. A new weighted proportional-fair resource method is presented by trading power consumption and communication latency in non-real-time applications. Performance analysis of the proposed architecture confirmed its energy efficiency, economic soundness, reliability, and environmental friendliness. Additionally, the suggested method was shown to increase the battery life of the end devices.

Keywords: HetNet; green communication; cellular network; solar PV; biomass generator; NRT; renewable energy

Citation: Hossain, M.S.; Islam, K.Z.; Alharbi, A.G.; Shafiullah, M.; Islam, M.R.; Fekih, A. Optimal Design of a Hybrid Solar PV/BG-Powered Heterogeneous Network. *Sustainability* **2022**, *14*, 2201. https://doi.org/10.3390/su14042201

Academic Editor: Adam Smoliński

Received: 28 December 2021
Accepted: 11 February 2022
Published: 15 February 2022

1. Introduction

The telecommunication sector of Bangladesh is growing at an exponential rate due to the rapid increment in mobile subscribers and the ever-increasing data demand. In other words, the nation is entering an era of very dense wireless networks with specialized needs such as tens of Gbps data rates and roughly 10 years of storage lifetime for low-power Internet of Things (IoT) devices [1,2]. The fast and widespread deployment of cellular base stations throughout the world has considerably increased energy consumption, thus depleting fossil fuel reserves and increasing greenhouse emissions (GHG). Furthermore, improved energy efficiency (EE), strong connection, and very low latency are projected

to make 5G networks attractive, particularly for delay-sensitive and mission-critical applications [1,2]. Modern cellular networks must be developed in such a way as to meet the challenges of future demands [3]. The next phase is expected to come in the area of IoT technologies. IoT connections are expected to rise to 26.9 billion by the end of 2026 [3]. Overall, global mobile data traffic is expected to grow from roughly 51 exabytes (EB) per month in 2020 to over 226 EB per month in 2026. Other important factors for this huge number of users are the Quality of service (QoS) and the vast volumes of data demand. Heterogeneous networks (HetNets), i.e., networks offering a combination of a variety of wireless coverage zones, are cellular platforms addressing the fast-increasing traffic intensity. HetNets have to be built to cope with changing scenarios such as performing simultaneous activities of the macro-, micro-, pico-, and femtocells [4,5]. That is a radius that typically covers 5–30 km, 1–2 km, 200 m, and 10 m for macro-, micro-, pico-, and femtocells, respectively [4,5]. The coverage distance may vary depending on the frequency band, terrain, and physical obstacles. These cells use a proportionate amount of power along with coverage. Approximately 1.5 million 5G base stations and 6 million 4G base stations are now operational throughout the world [6]. Recently, telecom networks have been offering a range of applications that are shaping the modern world. Nowadays, a major topic is the widening deployment and monitoring of IoT devices. Moreover, IoT applications are near-future applications in industry, agriculture, health, education, transportation, finance, and the environment [7,8]. The third-generation partnership project (3GPP) uses a radio technology standard called narrowband IoT (NB-IoT) to allow internet connectivity in a huge number of low-performance devices [9,10]. This NB-IoT standard may be used to prolong battery life using the discontinuous reception (DRX) mechanism.

Cellular base stations consume about 57% of the energy of the cellular networks, making them major energy users [11]. The energy consumption and greenhouse gas emissions of cellular networks are estimated to be roughly 130 TWh and 110 MtCO2e per year, respectively. When mobile phone emissions are added, the overall annual carbon footprint reaches the vicinity of 200 MtCO2e [3]. This amount has been growing at a 10% annual rate [12]. The international energy agency (IEA) has predicted in its 2018 world energy outlook (WEO2018) a 27% increase in global energy consumption from 2017 to 2040, which is equal to 3743 million tons of oil [13]. According to [14], the information and communication technology (ICT) sector consumes roughly 5% to 10% of the worldwide electrical generation and contributes about 2% to 4% of the global CO_2 emissions. Moreover, the worldwide reserves of coal, oil, and natural gas continue to decrease drastically, triggering the need for alternative energy sources, such as RES [15–17]. However, maintaining a high quality of service while lowering costs is a challenging problem for mobile industries. Powering BSs using locally available renewable energy sources is a potential solution to the problem. Efficient use of renewable energy is therefore one of the key priorities for the mobile industry to reduce costs and emissions while guaranteeing QoS. Consequently, it is necessary to incorporate sources of locally available RESs with conventional energy/electrical grid systems [15–17].

Overall, harvesting energy from locally accessible renewable energy sources is becoming a popular and established technique. Firstly, it lessens the reliance on fossil fuels as a sole source of energy. Secondly, these sources are abundant all around the globe. Thirdly, by lowering power generation costs and lowering carbon content, a large quantity of green energy may be harvested from renewable energy sources. Despite the above benefits, there are significant problems associated with generating energy, such as weather conditions and the dynamic nature of renewable energy sources, which can result in energy shortages or outages and negatively impact the QoS. However, combining multiple sources by integrating renewable energy sources with nonrenewable energy sources and suitable energy storage devices can improve QoS. The primary goal of the renewable-energy-powered cellular BS is currently to produce a green mobile communication framework with a minimum net cost.

The main focus of this paper is to develop an energy-efficient hybrid supply system to power the green cellular network in Bangladesh, taking into account the locally accessible renewable energy sources. Its main contributions are as follows:

- It proposes a hybrid solar PV and biomass-based energy supply system with enough energy storage devices for the long-term powering of heterogeneous cellular networks.
- Using HOMER optimization software, it investigates the techno-economic viability of the proposed architecture in the context of various system bandwidths.
- MATLAB-based Monte-Carlo simulations were used to evaluate the network's performance in terms of data rate and energy efficacy while considering dynamic traffic profiles.
- In contrast to previous concepts [18], it proposes a sleep mode mechanism to schedule bandwidth for NRT as well as IoT applications, thus resulting in considerable power savings and acceptable delays.

The remainder of the paper is organized as follows. A comprehensive review of the relevant literature is included in Section 2. The proposed HetNet architecture is detailed in Section 3. The cost modeling and optimization formula for the hybrid supply system are described in Section 4. The performance of the HetNet architecture is assessed in Section 5. Several key factors, including optimum system architecture, economic issues, wireless issues, and environmental issues are considered in the performance analysis. Conclusions are finally given in Section 6.

2. Literature Review

A growing interest in research is the effective use of renewable energy in cellular mobile technology. In addition, the future mobile industry will be strongly affected by the massive IoT devices deployment. Authors in [19,20] presented a solar PV-powered mobile base station in conjunction with sufficient energy storage devices. The technical and economic feasibility of the solar PV-powered cellular network has been examined thoroughly, taking into consideration the variation of solar radiation and traffic. In References [21,22], the authors used the HOMER platform to find the best system design and technical criteria for deploying hybrid solar PV/diesel generator (DG)-powered off-grid BSs across the world. The integration of solar PV with DG might reduce renewable energy output variations and increase the quality of service, but it partially increases DG-related issues, including high fuel prices, operation, and maintenance costs (OMC), and carbon emissions. In addition, fuel transfer to the DG is not economically efficient in remote regions. The combined utilization of multiple sources to achieve a sustainable and reliable energy source for BSs has been investigated in [23–25]. For a non-grid homogenous cellular network, a hybrid solar PV with a biomass generator (BG) supply scheme was developed in [26]. The integration of solar PV with biomass resources for establishing a long-term sustainable and reliable power station has been thoroughly investigated in reference [27]. In this work, the fundamental problems of developing a hybrid solar PV/biomass-focused power plant were investigated, and several significant solutions were proposed. A hybrid solar PV/wind turbine (WT)-powered macro-BS has been suggested in [28] considering the dynamic profile of renewable energy sources in Bangladesh. The works [25] and [29] employ a network with and without an energy sharing framework for the installation of the hybrid solar PV and WT-enabled homogenous network. Combining renewable energy with storage devices can improve reliability and minimize the energy gap between demand and supply, as shown in reference [30]. Being inspired by the potential benefits of renewable energy, Nokia Siemens has installed a hybrid solar PV/WT-powered base station in an urban location in Germany [31].

In References [29,32,33], energy sharing among neighboring base stations has been employed using resistive power lines or the intelligent grid. Average energy affinity (AEA) and stochastic energy affinity (SEA) measures are used to develop agglomerative and divisive hierarchical clustering algorithms to provide BSs with an energy-sharing model [29]. To achieve a fair decrease in energy usage and emissions of GHGs, a renewable energy-based community energy plan has been developed in [34]. In [35], the researchers reported

an optimal common solar PV framework throughout society. Reference [32] proposes an optimum energy cooperation architecture among cellular BSs, which incorporates both renewable energy and grids via physically linked resistive power lines. A macro-BS energy collaboration model is shown in reference [33]. According to the aforementioned research articles, onsite green energy exchange amongst BSs is cost-effective and sustainable.

Traditional macrocell designs are often built to cater to broader spectral regions, which frequently fail to provide the throughput required to provide smooth broadband service to uplink customers. Furthermore, users often move away from the macro-BS, causing significant inter-cell interference. Under the typical macrocell scenario, the lack of interior infiltration and the formation of dead patches significantly limit indoor coverage. Heterogeneous networks provide considerable network performance leaps through larger network capacity and improved coverage as a potential way to tackle these difficulties [4,5,36]. HetNet is a multi-tier cellular network in which macro-base stations serve as mother base stations and offer a consistent coverage area. Here, micro-and pico/femtocells serve as supporting BSs, consuming less energy due to their lower coverage area. As a result, HetNets can increase frequency reuse, and the different cells create hotspots that reduce the lack of cellular network coverage in dead places, saving energy and expanding the coverage area. Reference [36] describes a load-balancing approach that can help to improve HetNets' ranges.

The tradeoff between multiple QoS criteria for individual applications may be optimized using an effective resource scheduling technique. Reference [37] developed a minimum assured resource scheduling technique for NRT users. Reference [38] has provided a queue-size-aware, channel-adapted, and buffer-aware (CABA) packet scheduling algorithm. However, this solution cannot make use of all of the benefits of the popular proportional fair (PF) scheduler. Authors in [39] proposed a radio resource allocation architecture to assure proportionate fairness among the end-users. The impacts of the DRX setting on UE energy savings and delay were investigated by the authors in [40,41]. As seen in [42], Nokia has performed research on industrial DRX. It is generally understood that a tradeoff is always present between power savings and delay. Numerous DRX techniques are introduced in [43,44] to optimize the tradeoff.

3. System Description

This section provides a brief description of renewable energy resources in Bangladesh followed by a brief description of the system.

3.1. Opportunities and Potential of Renewable Energy in Bangladesh

The chosen location for this work is Bangladesh's rural areas since it provides the enormous potential of generating electricity from locally accessible RESs. Some of the most commonly available sources in Bangladesh are solar, wind, hydro, and biomass [45]. A brief description of the potential of solar and biomass (agricultural leftover) energy in Bangladesh is provided below.

3.1.1. Solar PV Energy

Bangladesh is a tropical country that lies between 20′′34′ and 26′′38′ North Latitude and 88′′01′ and 92′′41′ East Longitude. The country has a lot of potential for harvesting renewable energy from the sunlight. The daily average solar radiation of Bangladesh is 4.59 kWh/m^2/day, while solar intensity remains in the range of 4–6.5 kWh/m^2/day, according to NASA's database [14]. Bangladesh has the potential to receive around 70 PWh of solar energy annually, which can fulfill the entire country's electrical load [46]. Standalone solar PV-powered base stations are already deployed as a result of the aforesaid prospective solution. According to the authors of [20], in Bangladesh, around 521 solar PV-powered base stations were installed in the year 2015, and telecom companies are working to increase that number.

3.1.2. Biomass Energy

Bangladesh has a lot of biomass resources that might be used to generate electricity. Agricultural residue, animal dung, chicken droppings, and other biomass sources are the most readily available in the country. Agricultural residue is the most available resource for biomass in this agricultural country, with rice husk playing a key role. As per Bangladesh's 'Rice Mills Owners Association', the country has roughly 540 rice mills, each with a capacity of 30 tons per day and the potential to produce 171 MW per day [47,48]. In fiscal year (FY) 2012–2013, roughly 90.21 million tons of biomass were accessible in Bangladesh, with a 1344.99 PJ energy potential, which is equivalent to 373.71 TWh of electrical energy [49]. Reference [50] forecasts that Bangladesh will be capable of generating 7682 GWh of energy from rice husk in 2030.

3.2. System Description

Figure 1 depicts the schematic diagram of the proposed HetNet driven by the grid-tied hybrid solar PV/BG system. HetNet comprises different types of BSs equipped to meet the necessary data demands and has a specific size and power consumption. In general, a narrow area covering a small-size BS needs low-radiated power. The pico- and femto-BSs are therefore supplied with standalone solar PV, which consumes little power. A battery bank is linked to guarantee a constant energy supply, to counteract the RES deficiency or failure. The energy supply is regulated by an energy management unit (EMU) for each base station.

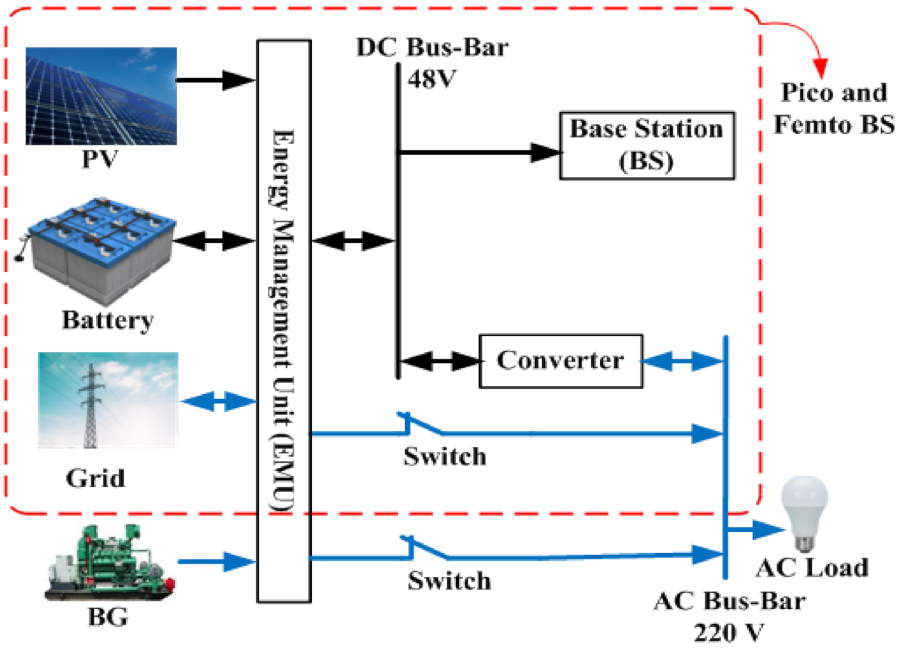

Figure 1. Architecture of the proposed system.

The major components of the system along with their mathematical models are briefly described below.

3.2.1. Solar PV System

The solar photovoltaic module harnesses the energy from the sun and converts it into electric energy. Based on the specifications and capital cost, a 'Sharp ND-250QC' model is considered for this work. The generated energy from the sun can be expressed as follows [51]:

$$E_{PV} = R_{PV} \times PSH \times \eta_{PV} \times 365 \text{ day/year} \quad (1)$$

where R_{PV} is the rated size, and PSH is the peak solar hour to average direct sunlight per day in kWh/m^2/day.

3.2.2. BG System

The average biomass availability of the selected region is 9 tons per day. The amount of power and energy generated from a biomass generator is given by Equations (2) and (3), respectively [49,52]:

$$P_{BM} = \frac{T_{BM}(tons/year) \times CV_{BM} \times \eta_{BM} \times 1000}{365 \times 860 \times (operating\ hour\ per\ day)} \quad (2)$$

$$E_{BM} = P_{BM}(365 \times 24 \times C_f) \quad (3)$$

where C_f corresponds to the ratio between the actual and maximum energy achievable, known as the capacity factor.

3.2.3. Storage System

The backup capacity of the battery storage depends largely on the autonomy. The duration of supply provided by the battery bank without outside support may be calculated as follows [51]:

$$B_{Aut} = \frac{N_{Batt} \times V_{nom} \times Q_{nom}(1 - \frac{SOC_{\min}}{100})(24\ \mathrm{h/day})}{P_{BS}} \quad (4)$$

where V_{nom} is the nominal voltage of a single battery (V), Q_{nom} is the nominal capacity of a single battery (Ah), and the battery $SOC_{\min}$ indicates the lower threshold limit of the battery's discharge [51]:

$$L_{Batt} = \min\left(\frac{N_{Batt} \times Q_{Lifetime}}{Q_{Thrpt}}, R_{Batt,f}\right) \quad (5)$$

where L_{Batt} is the lifetime throughput of a single battery (kWh), $Q_{Lifetime}$ is the annual throughput (kWh/year) of the battery, and $R_{Batt,f}$ is the float life of the battery bank in a year.

3.2.4. BS Load System

The optimal size of the hybrid supply system depends mostly on the cellular network's power demand. The overall energy consumption of a base station can be expressed as follows [53,54]:

$$\begin{array}{ll} P_{in} = M_{\mathrm{sec}}(P_1 + \Delta_p P_{\max}(\chi - 1)) & \text{If } 0 < \chi \leq 1 \\ = M_{\mathrm{sec}} P_{sleep} & \text{If } \chi = 0 \end{array} \quad (6)$$

where $P_1 = P_0 + \Delta_p P_{\max}$ represents the peak power consumed by the BS, Δ_p is the power slope depends upon the load, P_0 is the power consumed at the idle state, P_{sleep} is the power drawn at sleep mode, and χ represents traffic load. The base station parameters along with the power consumed by the major components of the BSs from different system bandwidths are obtained from references [53,54].

3.2.5. Power Grid

The power grid is typically an interconnected structure that delivers power to the load. In this study, the suggested hybrid solar PV/BG system supplies surplus power to the grid.

3.3. Energy Sharing Model

If the case is an on-grid condition, energy can be shared between a network connection system and the electrical grid system. The algorithm of the proposed system is illustrated using the flowchart in Figure 2. Three separate scenarios occur for the state of the grid.

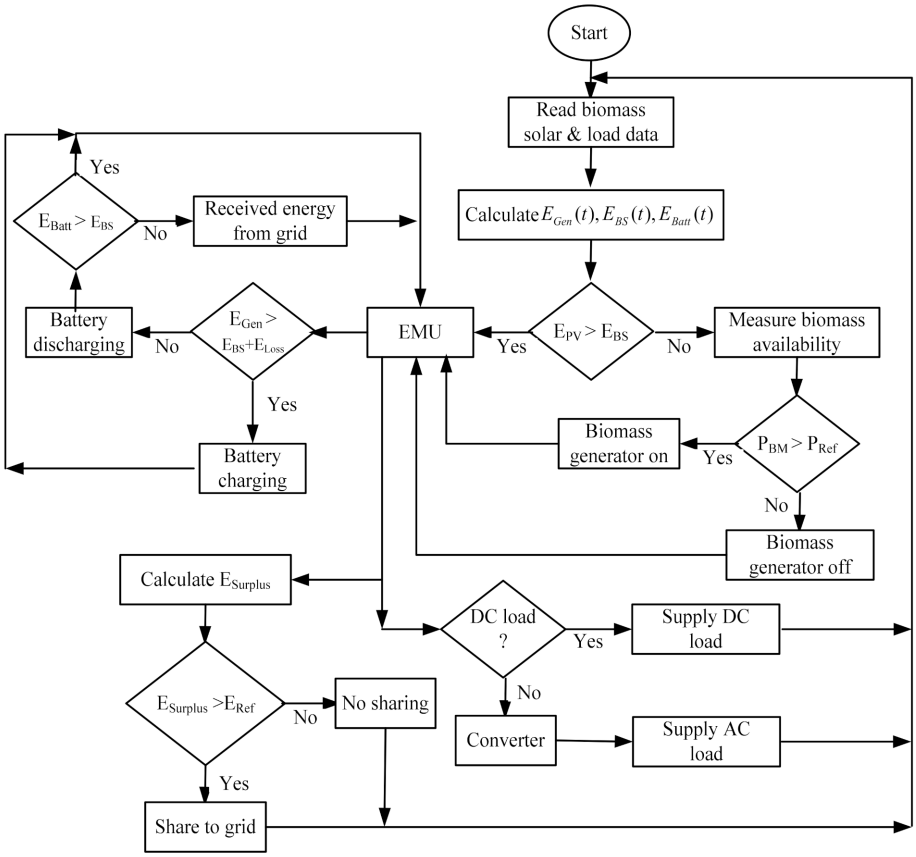

Figure 2. Flow chart of the proposed system.

Case I: Generation is higher than demand ($E_{Gen} > E_D$):

If $E_{Gen} > E_D$, the green energy is enough to meet the BS's own need for energy. Surplus energy is stored in the battery bank for backup power supply and energy for sharing. The amount of energy share and the loss of power supply probability of the system can be expressed as follows:

$$E_{Share} = E_{Gen} - E_{BS} - E_{Losses} \tag{7}$$

$$LPS(t) = 0 \tag{8}$$

where E_D is the summation of E_{BS} and E_{Loss}, and LPS represents the loss of power supply probability. A reliable system must have an LPS that is either zero or greater than zero.

Case II: Generation is equal to demand ($E_{Gen} = E_D$):

If $E_{Gen} = E_D$, then the green electricity generated is supplied to the base station, and the battery bank is ready to provide backup power, which means $E_{Share} = 0$, $LPS\ (t) = 0$.

Case III: Generation is lower than demand ($E_{Gen} < E_D$):

If $E_{Gen} < E_D$, the harvested green energy cannot fully meet the BS energy need. Therefore, backup power is provided by the battery bank, and the remaining energy is received from the electrical grid.

3.4. Wireless Performance Metrics

The wireless network performance is measured using throughput and energy efficiency measurements. The total achievable throughput ($R_{total}(t)$) of the network can be expressed as follows [30]:

$$R_{total}(t) = \sum_{k-1}^{U} \sum_{i=1}^{N} BW \log_2(1 + SINR_{i,k}) \tag{9}$$

where N is the number of BSs, U is the number of end-users, and $SINR_{i,k}$ is the received signal-to-interference-plus-noise-ratio at the kth end-users served by base station BS_i.

The ratio of total power and network power consumption can be expressed as energy efficiency (EE). The EE metric at time t can be represented by [25]:

$$\eta_{EE} = \frac{R_{Total}(t)}{P_{BS}(t)} \tag{10}$$

where $P_{BS}(t)$ is the total power consumed in all BSs at time t and can be calculated using Equation (6).

3.5. Resource Scheduling

In long-term evolution (LTE), especially for non-real-time (NRT) or IoT applications, the discontinuous reception (DRX) mechanism has been implemented to optimize the end-users' battery lifetime. However, power consumption and wake-up delays are always trade-offs for end users. Consequently, the optimization of the DRX mechanism is required. A modified DRX Algorithm targeting NRT applications is suggested. This latter aims at improving battery life whilst achieving permissible delays. Without the DRX mechanism, user equipment had to continuously be in the 'ON' state, even if there is no traffic, which increases battery consumption drastically. The algorithm describes the communication state between BS and IoT applications. An inactivity timer starts after the end of the 'ON' state (active data transfer). When the inactivity timer advances to its expiration with no UL/DL data transfer request, the sleep mode mechanism will start again.

The current DRX model initiates through short sleep time (τ_S). If it can end successfully without any UL packet arrival or DL packet arrival during paging, long sleep time (τ_T) initiates. On the other hand, the proposed DRX mechanism initiates a sleep time interval that keeps growing from a short to long cycle timer with a step size τ_{ST}. If, throughout this time, data transfer requests arrive, the fall will be followed by a rise again. Here, a number of cycles (n) are needed to reach from τ_S to τ_L or vice versa. However, once the UL packet transfer request has been detected within the DRX period or the DL/UL packet transfer request has been detected within the paging interval, an instant on period timer will initiate, and the sequence will keep rotating. The algorithm of the proposed DRX mechanism is depicted in the flowchart of Figure 3.

Here, an M/G/1 queue model has been used to model the packet arrival and service rate, Markovian (Poisson process) for the packet arrival rate (λ), general distribution for service rate (μ), and the server is singular. The equation for calculating the percentage of power-saving calculation has been modified from [55]:

$$P_{Save}(\%) = [1 - [\frac{E[T_{Data}]}{E[T_{Total}]} + \frac{P_{Watt} \times E[T_{Watt}]}{P_{Data} \times E[T_{Total}]} + \frac{P_{OFF} \times E[T_{OFF}]}{P_{Data} \times E[T_{Total}]}]] \times 100 \tag{11}$$

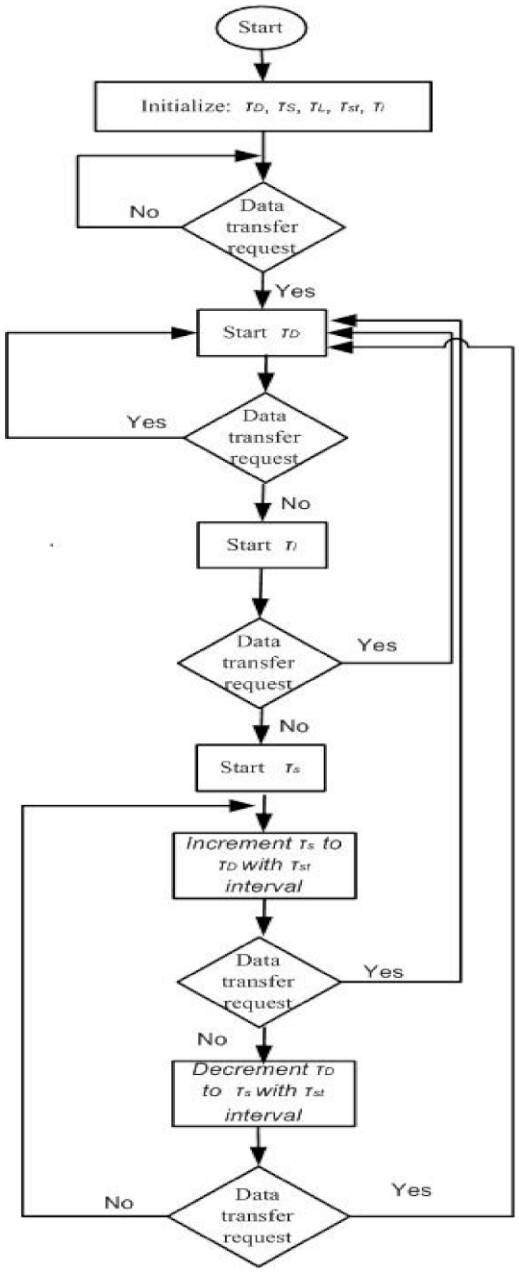

Figure 3. Proposed sleep algorithm for IoT applications.

4. Simulation Setup, Cost Modeling, and Optimization

4.1. Simulation Setup

The project lifetime and the yearly interest rate were assumed to be 20 years and 6.75%, respectively, for the HOMER simulation set-up, which shows the long-term viability of the proposed system. Furthermore, solar panel double-axis tracking is modeled, and appropriate battery storage is linked to supply the BS load requirement. To meet the energy demand of the BSs and to ensure backup power at a reduced net present cost, HOMER optimization software is used. Figures 4 and 5 illustrate the HOMER layout of the system for macro-, micro-, pico-, and femto-BSs under 10 MHz bandwidth. The base stations are mainly DC load, and it varies over time due to the dynamic character of the traffic intensity. It also consists of a 30W AC lamp, and with the continuous use of the light from 6 p.m. to 6 a.m., the AC load stays constant. Table 1 presents the technical parameters along with their respective values for the HOMER simulation configuration. The following are the

system's parameters of the renewable energy sources: Solar radiation: 4.59 kWh/m^2/day; Biomass availability: 9 tons/day. The interest rate is 6.75%.

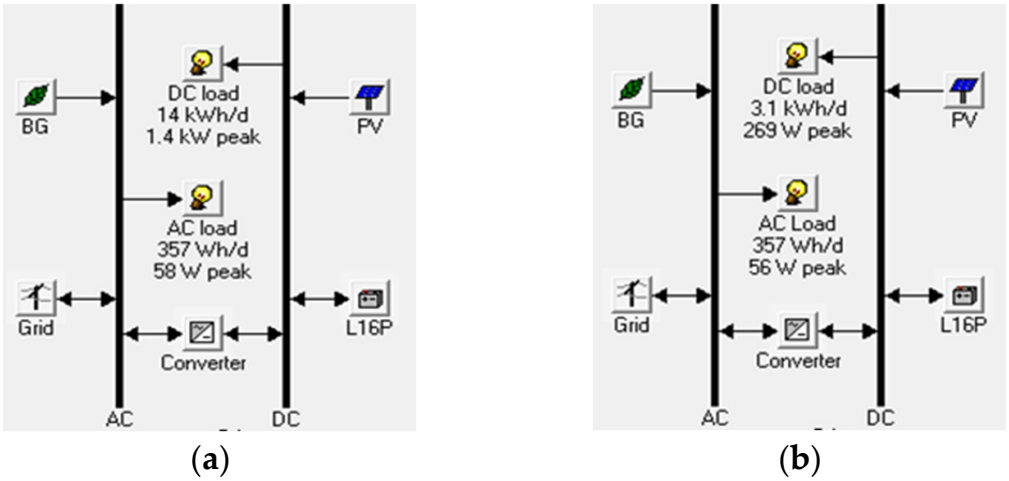

Figure 4. Layout in HOMER under 10 MHz system BW (macro and micro): (**a**) For macro BS; (**b**) For micro BS.

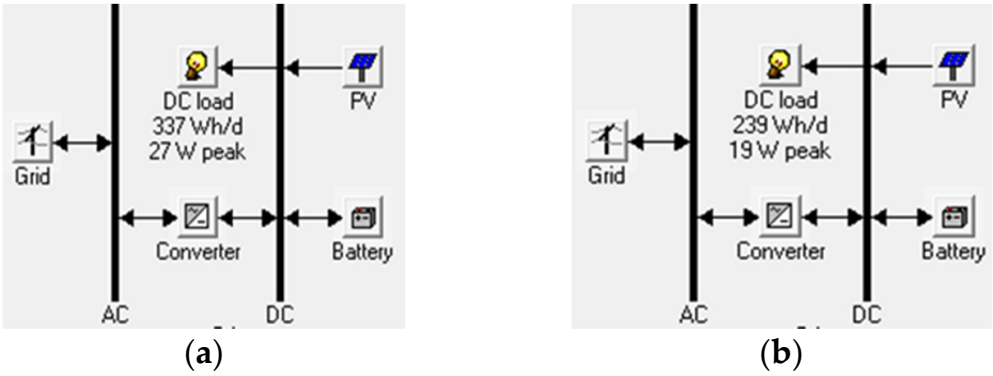

Figure 5. Layout in HOMER under 10 MHz system BW (pico and femto): (**a**) For pico BS; (**b**) For femto BS.

Table 1. HOMER simulation parameters and specifications [49,51,52].

Components	Constraints	Value
Solar PV	Operational lifetime	25 Years
	Derating factor	90%
	System tracking	2-Axis
	CC	USD 1000/kW
	RC	USD 1000/kW
	OMC/Year	USD 10/Year
Biomass Generator	Efficiency	30%
	Operational lifetime	25,000 Hours
	CC	USD 600/kW
	RC	USD 600/kW
	OMC/Year	USD 0.05/Hour
	FC	USD 30/Tone
Electrical Grid	Energy purchase price	USD 0.122/kWh
	Energy sellback price	USD 0.110/kWh
	Demand charge	USD 0.350/kW/Month

Table 1. *Cont.*

Components	Constraints	Value
Battery	Round trip efficiency	85%
	BSOCmin	30%
	Vnom	6V
	Qnom	360 Ah
	Lifetime throughput	1075 kWh
	CC	USD 300/Unit
	RC	USD 300/Unit
	OMC/Year	USD 10
Converter	Efficiency	95%
	Operational lifetime	15 Years
	CC	USD 400/kW
	RC	USD 400/kW
	OMC/Year	USD 10/Year

4.2. Cost Modeling

The net present cost (NPC) is the summation of associated costs (such as capital cost (CC), replacement cost (RC), operation and maintenance cost (OMC), fuel cost (FC), and salvage value (SV) that arise within the entire project. The use of biomass in biomass generators involves a significant fuel cost, and the NPC of the suggested system can be expressed as follows [51]:

$$\text{NPC} = \frac{\text{TAC}}{\text{CRF}} = \text{CC} + \text{RC} + \text{OMC} + \text{FC} - \text{SV} \tag{12}$$

The acronyms TAC and CRF are the total system cost and recovery elements annually that can be computed using (12) and (13) [51]:

$$\text{TAC} = \text{TAC}_{\text{CC}} + \text{TAC}_{\text{RC}} + \text{TAC}_{\text{OMC}} \tag{13}$$

$$\text{CRF} = \frac{i(1+i)^N}{(1+i)^N - 1} \tag{14}$$

where N is the project's lifespan and i the real yearly rate. Rescue values are called the costs after the endeavor and are estimated by the following equation [51]:

$$\text{SV} = C_{RC}\left(\frac{C_{RL}}{C_L}\right) \tag{15}$$

where C_{RC},C_{RL}, and C_L are the replacement cost, remaining lifetime, and lifetime of the component, respectively.

The cost of energy (COE) is a metric that measures the cost of producing a unit of electricity, which is expressed in dollars per kilowatt-hour (kWh) as follows [51]:

$$COE = \frac{\text{NPC} \times \text{CRF}}{E_{Gen}} \tag{16}$$

4.3. Optimization

The challenge of designing a hybrid renewable energy generation model is stated as an optimization problem that has the goal of decreasing NPC while taking into account a variety of schemes and operation limitations. The major objective of this research is to reduce NPC by minimizing energy shortages/outages and grid pressure by maximizing the use of renewable energy. The objective function of the system is expressed as follows [25]:

$$\begin{aligned} &\textit{Minimize} && \text{NPC} \\ &\textit{Subject to} && E_{PV} + E_{BG} > E_{BS} && \text{(17a)} \\ & && E_{PV} + E_{BG} + E_{Batt} = E_{BS} + E_{Losses} && \text{(17b)} \\ & && E_{Surplus} = E_{Gen} - E_{BS} - E_{Losses} && \text{(17c)} \\ & && E_{Batt\min} \leq E_{Batt} \leq E_{Batt\max} && \text{(17d)} \end{aligned}$$

where (E_{Losses}) is the summation of losses from converter and battery. The complementary effect of solar PV and biomass generators can fulfill the base station energy demand and ensure 100% energy availability as presented in constraint (17a). The combined utilization of solar PV and BG in addition to battery storage can supply the load requirement and associated losses as stated in constraint (17b). According to constraints (17c), a certain percentage of surplus electricity is put in storage in the battery, and the remaining portion is conveyed to the electrical grid. The constraint (17d) specifies that the storage capacity must not exceed the upper edge nor fall below the lower limit.

5. Performance Analysis

Several key factors, including optimum system architecture, economic issues, wireless issues, and environmental issues, are highlighted in this section. The HOMER is chosen to analyze the proposed hybrid supply system's optimal design and technical requirements for on-grid situations to minimize the cost of electricity and greenhouse gas emissions over 20 years. Using MATLAB-based Monte Carlo simulations, the wireless network was fully assessed. Throughput and energy efficiency measures were considered as performance metrics.

5.1. Optimal System Architecture

Table 2 summarizes the optimal size of different components for diverse system bandwidths under average solar radiation. In the HOMER software, the simulation was performed considering the dynamical behavior of renewable sources and data traffic. Due to the growing quantity of energy consumption, a larger solar PV panel size is necessary for higher system bandwidths (for macro- and micro-BS). In addition, the optimal size of the other system components remains unchanged as system bandwidth changes. This means that the proposed system can satisfy the energy demand of the BS under various bandwidth situations without altering system components on a significant scale.

Table 2. Optimal system architecture of the gird-tied system under 10 MHz system BW.

BW (MHz)	PV (kW)				BG (kW)				Battery (units)				Converter (kW)			
	Macro	Micro	Pico	Femto	Macro	Micro	Pico	Femto	Macro	Micro	Pico	Femto	Macro	Micro	Pico	Femto
5	3	2	2.5	2.5	1	1	*	*	32	24	8	8	1.5	1.5	1.5	1.5
10	3	2.5	2.5	2.5	1	1	*	*	32	24	8	8	1.5	1.5	1.5	1.5
15	3.5	3	2.5	2.5	1	1.5	*	*	32	24	8	8	1.5	1.5	1.5	1.5
20	3.5	3	2.5	2.5	1	1.5	*	*	32	24	8	8	1.5	1.5	1.5	1.5

* Not applicable.

5.2. Energy Issue

The annual energy consumed (DC and AC load), surplus energy, and shared energy for the different networks with a 10 MHz bandwidth are summarized in Table 3.

Table 3. Individual energy breakdown under 10 MHz BW.

Items	Macro	Micro	Pico	Femto
AC load (kWh/Yr)	130	130	0	0
DC load (kWh/Yr)	5110	1117	123	87
Surplus energy (kWh/Yr)	637	574	847	858
Sold energy (kWh/Yr)	3172	3287	3982	4007

The monthly statistics of power contribution by the different supply systems are presented in Figures 6–9 for the macro-, micro-, pico-, and femto-base stations, respectively. Those figures were obtained using data considering the dynamic profile of renewable energy sources with an average solar intensity of 4.59 kWh/m^2/day and a 10 MHz system bandwidth. In line with our expectations, ideal renewables such as solar photovoltaics contribute more energy throughout the year. However, owing to the effective utilization of renewable energy, the biomass generator delivers less energy. It is also seen that no electrical grid energy was utilized for the maximal use of renewables. The fundamental purpose of the electric grid system is to sell the extra energy from renewables and to receive energy back in the event of a shortage or failure of renewable energy and storage system. The introduced system can decrease capital cost and carbon emissions since, under all situations, solar PV provides the most energy.

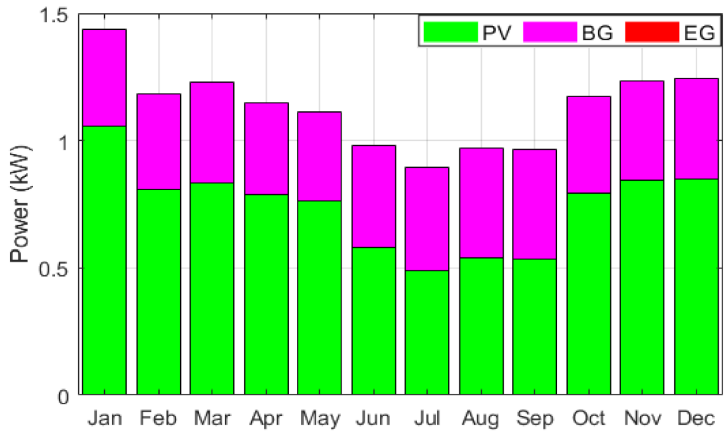

Figure 6. Monthly power contribution for macro-BS under 10 MHz system BW.

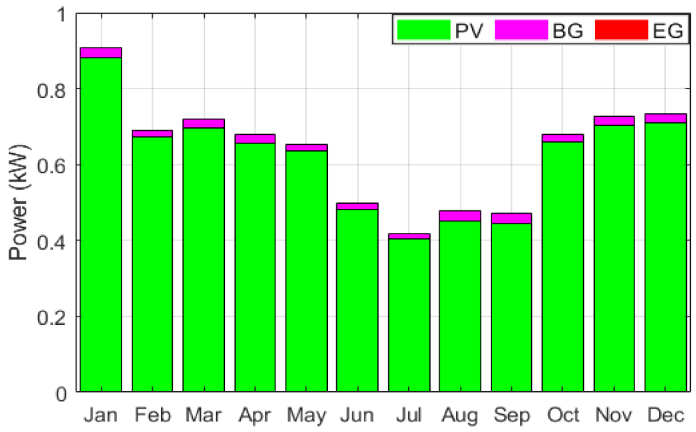

Figure 7. Monthly power contribution for micro-BS under 10 MHz system BW.

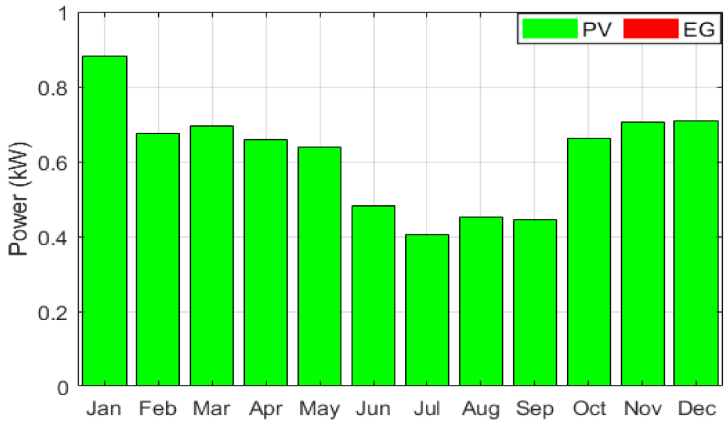

Figure 8. Monthly power contribution for pico-BS under 10 MHz system BW.

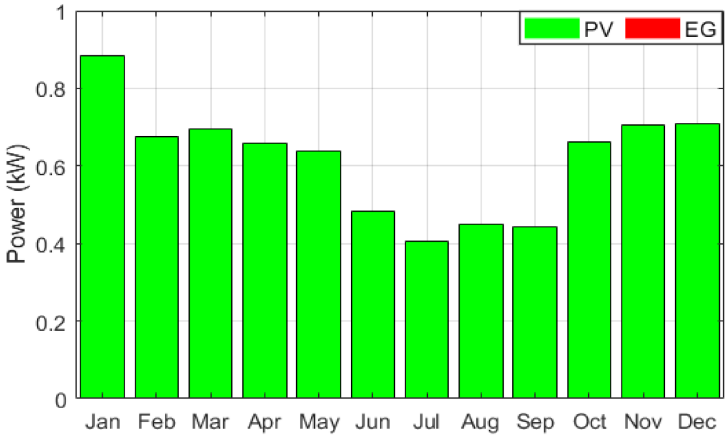

Figure 9. Monthly power contribution for femto-BS under 10 MHz system BW.

A comprehensive comparison of the yearly energy breakdown by the hybrid supply system under different system bandwidths are shown in Figures 10–13, for macro-, micro-, pico-, and femto-base stations, respectively. The following are detailed energy calculations for the 10 MHz system bandwidth from the solar PV panels, and biomass generators.

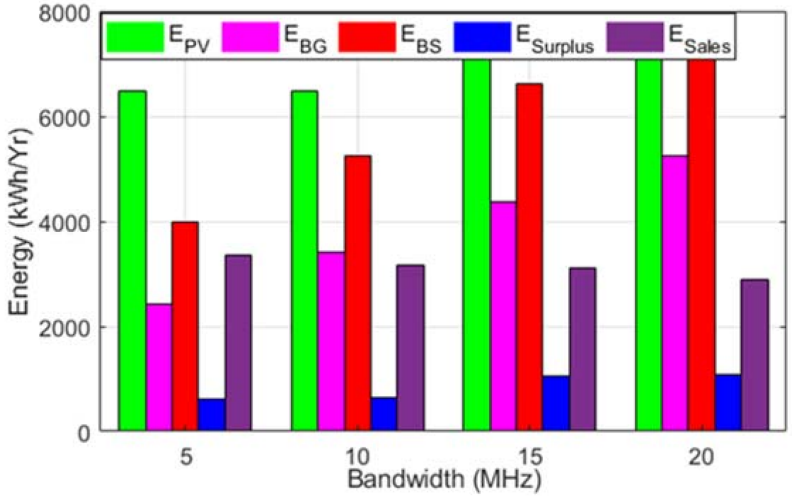

Figure 10. Individual energy breakdown for macro-BS.

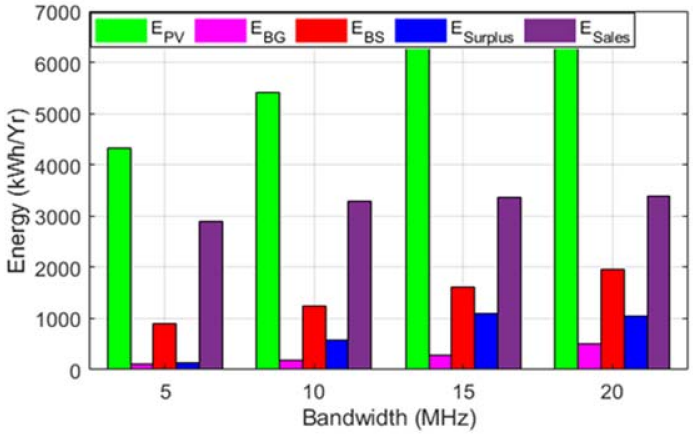

Figure 11. Individual energy breakdown for micro-BS.

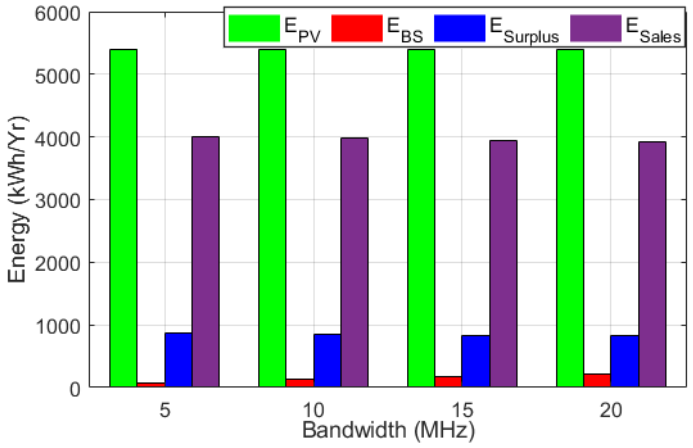

Figure 12. Individual energy breakdown for pico-BS.

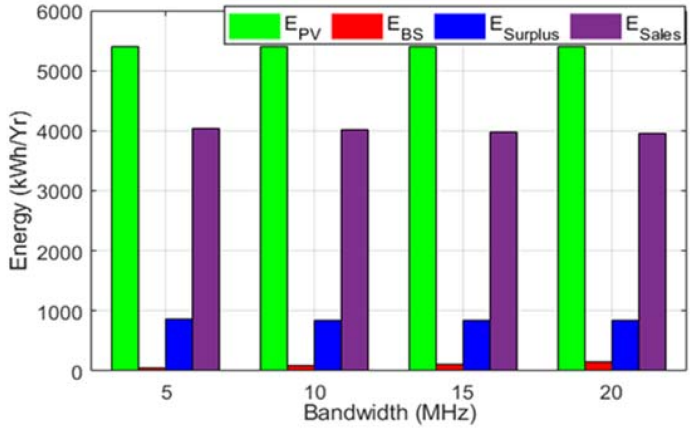

Figure 13. Individual energy breakdown for femto-BS.

Solar PV: As referred to in Table 2, the optimum size of the solar PV panel is 3 kW for the macro-BS system under a 10 MHz bandwidth. The year-round energy produced through the solar PV module can be approximated using (1): 3 kW × 4.59 × 0.9 × 365 days/year = 4523.44 kWh. Furthermore, due to the two-axis tracking mode, this value will be 6486 kWh.

Biomass Generator: The optimal size of the biomass generator is 1 kW. The running hours of the BG are 5342 h per year (14.632 h per day) and the used up bio-feedstock is 3.46 tones/year as obtained from HOMER simulation under macro-BS. Therefore, the

annual generated power is calculated using (2) as follows: P_{BG} = (3.46 tones/year (T_{BM}) × 3411.33 Kcal/Kg (CV_{BM}) × 0.30 (h_{BG}) × 1000)/(365 × 860 × 14.632 h (t_{op})) = 0.770 kW.

In contrast, the generated energy is assessed using (3) as follows: E_{BG} = 0.770 kW (P_{BG}) × 365 × 24 × 0.50 (capacity factor) = 3416 kWh/year for macro-BS, under 10 MHz bandwidth. In a similar procedure, the year-on-year energy produced by the other system configurations is computed.

The fuel of the biomass generators is organic feedstock. The amount of energy harvested from the solar PV/BG system is linearly related to the amount of bio-feedstock consumption and base station energy demand. The quantity of organic feedstock used by the hybrid solar PV/BG system under different system bandwidths is illustrated in Figure 14. It is observed that a larger quantity of biomass was used by the PV/BG solar system, which was linked to grid sharing. In particular, the networked system always generates higher energy than is necessary. The extra energy is therefore conveyed to the electrical network, which reduces grid pressures as well as the cost of capital through the maximum use of renewable energy sources.

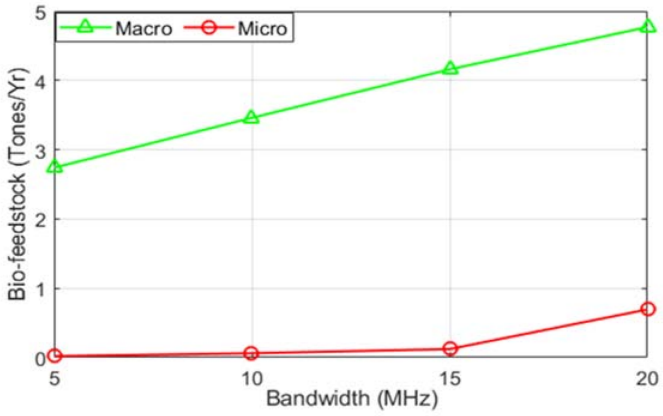

Figure 14. Biomass consumed for the proposed grid-tied system.

For a macro-base station under 10 MHz system bandwidth, the total number of batteries required is 32:8 in series and 4 in parallel to support the load demand in case of the shortage/failure of renewable energy. Due to better features of charge and discharge rate, the "Trojan L16P" battery has been selected. Using (4) HOMER determines the autonomy of the battery bank by 80.9 h. The yearly battery bank's autonomy under various network topologies is displayed in Figure 15. According to (5), the battery's throughput is proportional to the BS energy needs, while its autonomy is inversely proportionate. Therefore, the larger bandwidth of the system shows a lower battery autonomy value and a higher battery performance. Furthermore, a good battery bank modeling and the battery bank charge/discharge rating can enhance the reliability of the renewable-energy-driven supply system.

The monthly statistics of renewable energy sold to the electrical grid system under different network conditions are shown in Table 4. In line with our expectations, after meeting the needed energy demand of the BSs, the grid-connected hybrid solar PV/BG system may share a considerable amount of renewable energy with the power grid system. On the other hand, Figure 16 displays the sold energy at various system bandwidths. In the case of the macro-base station system, the solar PV/BG may return about 3172 kWh of energy per year, according to the data provided in Table 4, through the selling of excess energy to the electric grids system. It is also observed that in pico- and femto-base station cases, the amount of sold energy is comparatively higher due to the lower value of the load demand. However, the solar PV/BG system can transfer a greater amount of renewable energy to the grid, therefore reducing energy costs and grid pressure. Therefore, three objectives can be achieved with the energy generated: (i) A significant part of the energy generation is required to meet the BS load demand; (ii) in the battery system, a certain

amount of extra energy is kept to support the system during shortages/outage of renewable energy; (iii) to ensure the stability of the supply via a thoroughgoing use of renewable energy sources, the residual quantity of energy is conveyed to the electrical grid.

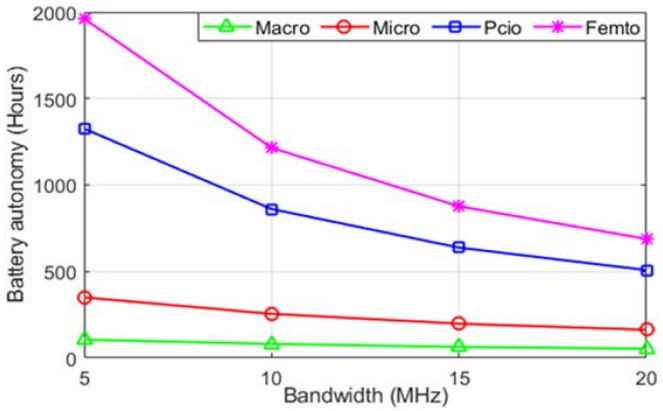

Figure 15. Battery autonomy for the proposed gird-tied system.

Table 4. Monthly statistics of sold energy by the HetNet under 10 MHz system BW.

Month\BS Type	Macro (kWh)	Micro (kWh)	Pico (kWh)	Femto (kWh)
January	393	395	424	426
February	276	277	324	326
March	318	322	376	378
April	292	315	374	376
May	291	306	368	370
June	188	206	279	281
July	148	163	238	241
August	170	192	266	268
September	176	186	252	255
October	309	315	373	375
November	299	300	349	350
December	311	310	359	361
Annual	**3172**	**3287**	**3982**	**4007**

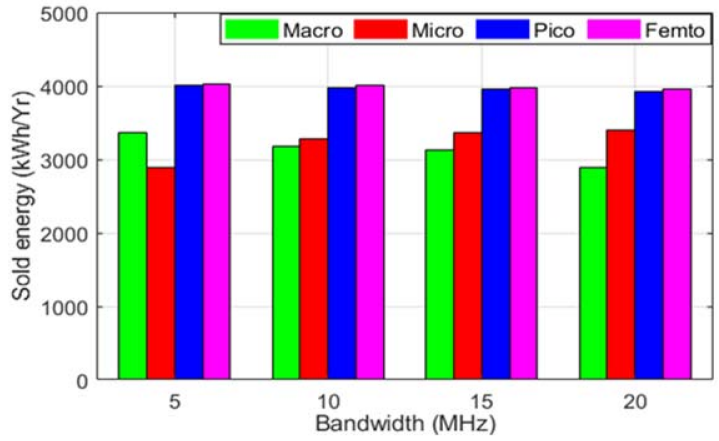

Figure 16. Energy sold to the electrical grid by the HetNet under different system BW.

5.3. Economic Issue

In order to build a cost-effective hybrid supply system, the results of the HOMER optimization software are used in this section to examine various expenses connected with the hybrid solar PV/BG system. Critical studies of these costs have been conducted, considering the dynamic character of renewable energy sources in various network topologies.

The nominal cash flow summary of the proposed system under a 10 MHz system bandwidth is shown in Figures 17–20 for macro-, micro-, pico-, and femto-base stations, respectively. The results were obtained by modeling the system in HOMER using the average solar radiation profile and biomass availability in the selected location. It is seen that, as compared to other types of components, the battery bank has a greater cost since the battery's lifetime is shorter than the project's term. It should be noted that the grid system has a negative NPC value because a larger volume of excess energy is sold to the grid.

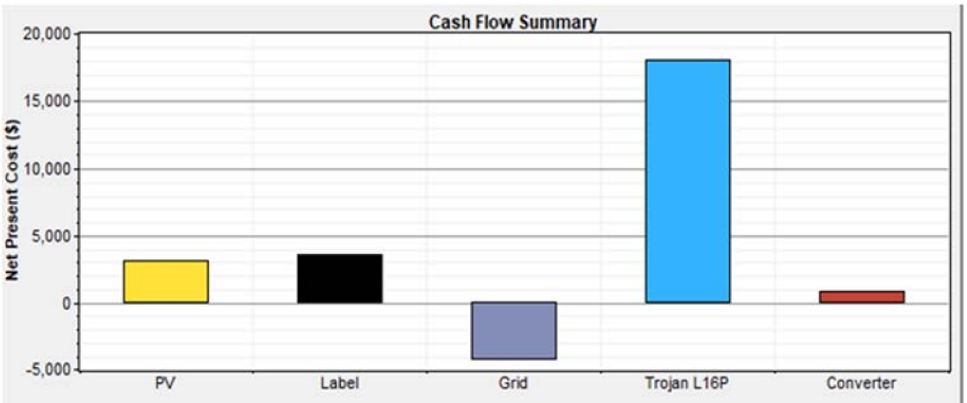

Component	Capital ($)	Replacement ($)	O&M ($)	Fuel ($)	Salvage ($)	Total ($)
PV	3,000	0	324	0	-162	3,162
BG	660	1,302	577	1,122	-130	3,532
Grid	0	0	-4,180	0	0	-4,180
Trojan L16P	9,600	4,996	3,457	0	0	18,053
Converter	600	225	162	0	-108	879
System	13,860	6,523	340	1,122	-401	21,445

Figure 17. Cash flow summary of the grid-tied hybrid solar PV/BG system under macro-BS.

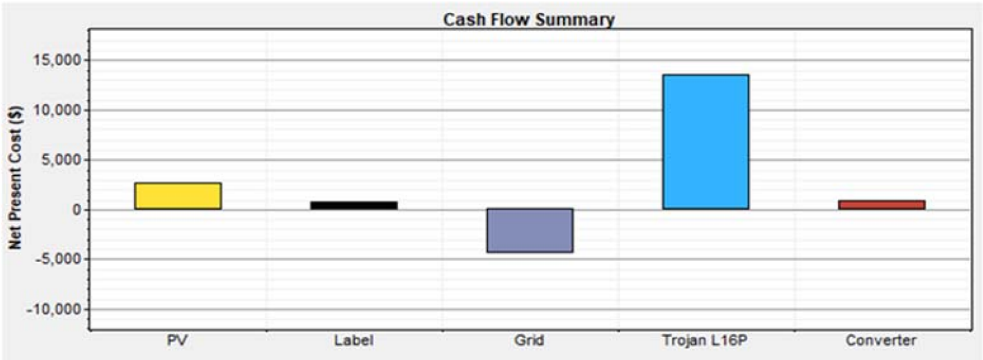

Component	Capital ($)	Replacement ($)	O&M ($)	Fuel ($)	Salvage ($)	Total ($)
PV	2,500	0	270	0	-135	2,635
BG	660	0	68	85	-89	723
Grid	0	0	-4,332	0	0	-4,332
Trojan L16P	7,200	3,747	2,593	0	0	13,539
Converter	600	225	162	0	-108	879
System	10,960	3,972	-1,240	85	-333	13,444

Figure 18. Cash flow summary of the grid-tied hybrid solar PV/BG system under micro-BS.

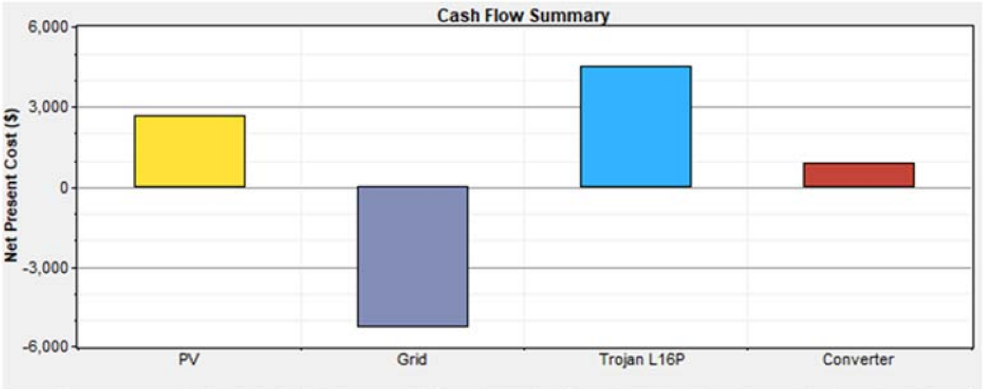

Component	Capital ($)	Replacement ($)	O&M ($)	Fuel ($)	Salvage ($)	Total ($)
PV	2,500	0	270	0	-135	2,635
Grid	0	0	-5,248	0	0	-5,248
Trojan L16P	2,400	1,249	864	0	0	4,513
Converter	600	225	162	0	-108	879
System	5,500	1,474	-3,951	0	-244	2,779

Figure 19. Cash flow summary of the grid-tied solar PV system under pico-BS.

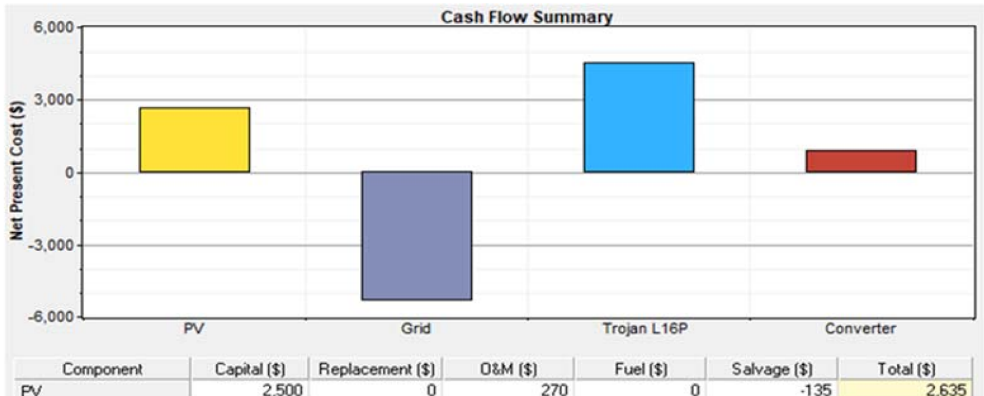

Component	Capital ($)	Replacement ($)	O&M ($)	Fuel ($)	Salvage ($)	Total ($)
PV	2,500	0	270	0	-135	2,635
Grid	0	0	-5,281	0	0	-5,281
Trojan L16P	2,400	1,249	864	0	0	4,513
Converter	600	225	162	0	-108	879
System	5,500	1,474	-3,985	0	-244	2,746

Figure 20. Cash flow summary of the grid-tied solar PV system under femto-BS.

Figure 21 depicts a comparison of NPC for the various network topologies. With the escalation of system bandwidth, all NPC curves are decreased linearly to meet the increased energy requirement. In addition, the NPC curve of the macro-BS system has a lower value as compared to the other system, which indicates that higher system bandwidth and energy trading strategy may decrease capital costs considerably. In this research on maximizing the use of renewable energy sources and increasing system dependability, the energy trading strategy for the grid is thoroughly studied.

The quantitative comparison of the per-unit capital cost of power generation in different network topologies of the proposed system is illustrated in Figure 22. Note that, in line with the theory, a reduced energy generation price value is achieved for the greater system bandwidth. In addition, the costs of generating electricity for the smaller system are greater than those of the larger size system because, as indicated previously, NPC is more involved in the larger base station.

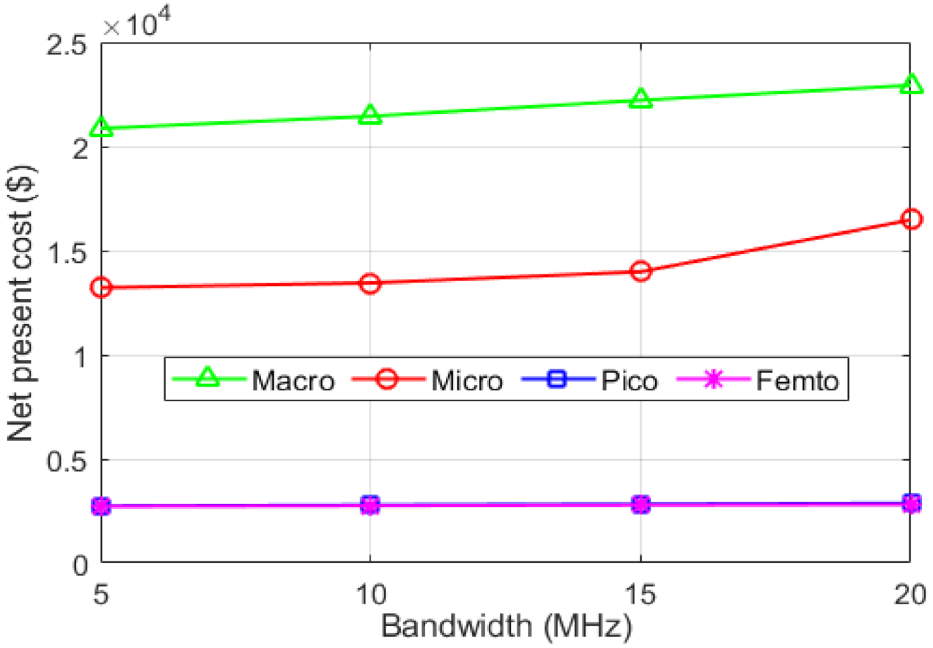

Figure 21. Net present cost of the HetNet under different system BW.

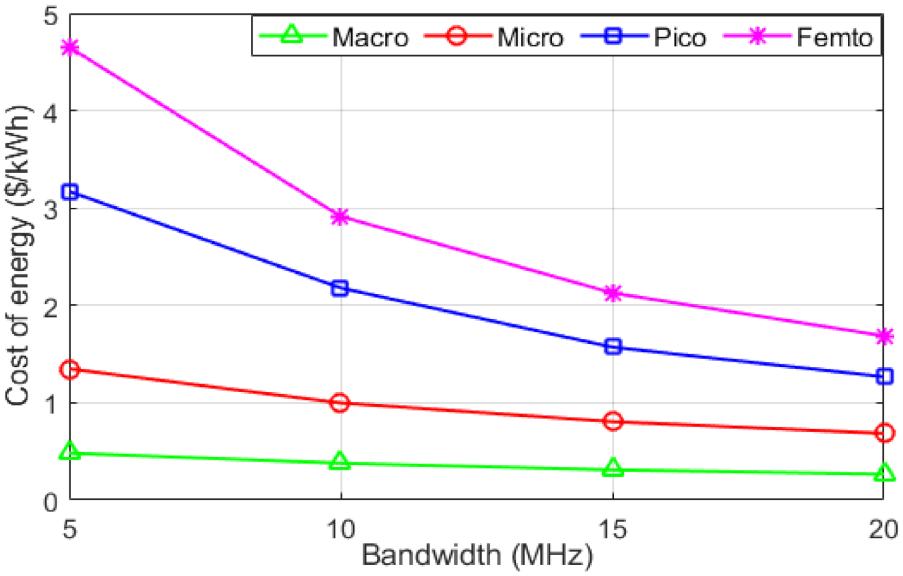

Figure 22. Cost of energy of the HetNet under different system BW.

5.4. Wireless Issue

The wireless network performance considering several system bandwidths is illustrated in Figures 23 and 24 respectively. The performance indicators were assessed in light of the two-tier LTE hexagonally shaped mobile network with 19 base stations. The throughput indicates the number of bits per second transferred. Instead, the word "energy efficiency" quantifies the number of bits sent per watt, equal to the ratio of overall throughput to the total output essential for the base station. A system that delivers higher throughput and energy efficiency performance is always desirable. Figure 23 demonstrates that the given system has enough throughput performance and is similar to the traffic intensity profile. In addition, the larger system bandwidth gives a better value to the output performance because of the higher energy consumption. As referred to in (10), the energy

efficiency is in a straight line related to the network's performance. This results in increased energy efficiency curves with an increase in bandwidth, as seen in Figure 24.

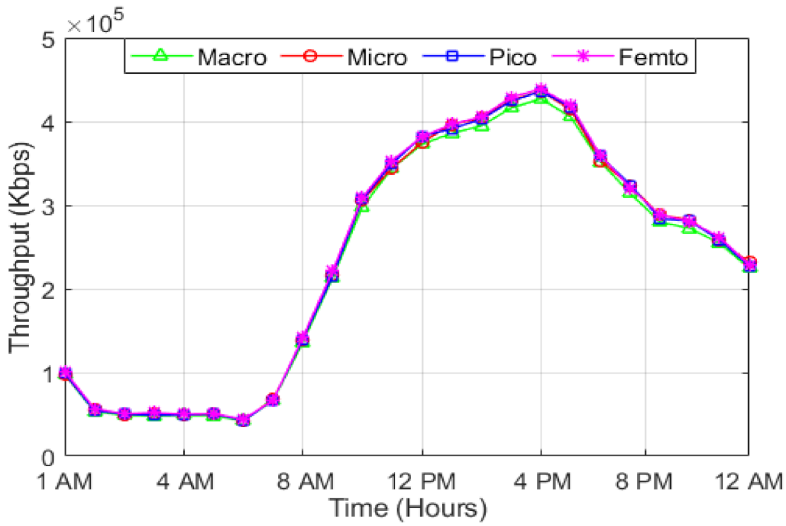

Figure 23. Throughput performance over 24 h under 10 MHz BW.

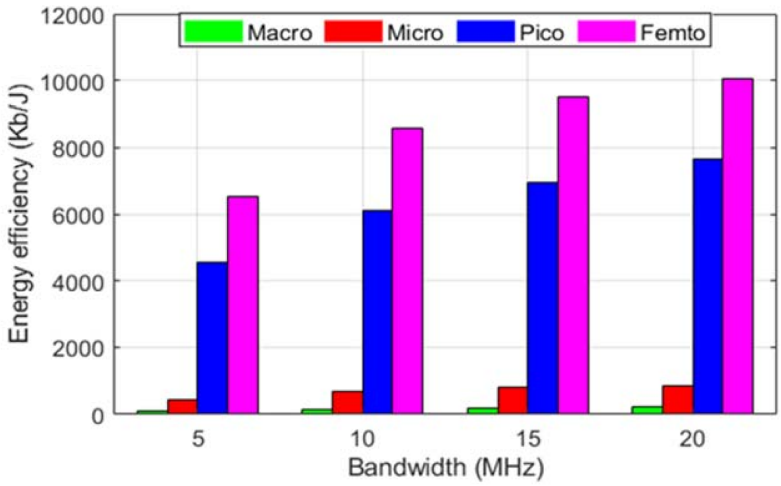

Figure 24. Energy efficiency for different system BW.

5.5. Environmental Issue

As an ideal renewable energy source, solar PV does not contribute to the emission of any carbon content, whereas the biomass generator releases a tiny amount of carbon content during the processing of the biomass [56]. Controlling waste from the biomass generator system and telecommunication equipment can help green mobile communication become more sustainable. The statistics for the emissions produced by the proposed system under different system bandwidths are shown in Figure 25. The emission statistics demonstrate a clear ratio with BG's organic feedstock consumption by increasing system BW. Table 5 summarizes the specifics of the pollutants released by the biomass generator with system bandwidth under 10 MHz. This pollution may be reduced to a minimum value with the introduction of new technology. The negative sign of the emissions implies that a grid-connected solar PV/BG system may considerably reduce carbon emissions by sharing extra green energy with the electrical grid. Finally, the suggested method may preserve the environment indirectly by lowering the use of rice husk (the major source of biomass), as demonstrated in Table 6.

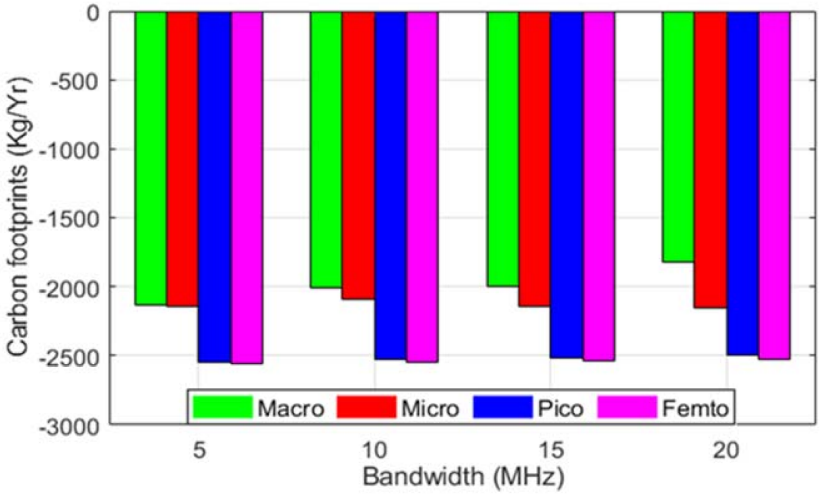

Figure 25. Carbon footprints for the different system BW.

Table 5. Carbon contents for the hybrid system under 10 MHz BW.

Carbon Particles	Values			
	Macro	**Micro**	**Pico**	**Femto**
Carbon dioxide	−1999	−2077	−2516	−2532
Carbon monoxide	0.0225	0.0017	0	0
Unburned hydrocarbons	0.00249	0.000189	0	0
Particulate matter	0.0017	0.000128	0	0
Sulfur dioxide	−8.69	−9.01	−10.9	−11
Nitrogen oxides	−4.05	−4.39	−5.34	−5.37
Total	**−2012**	**−2090**	**−2532**	**−2548**

Table 6. Emissions by different sources [50].

Fuels	Emissions (Kg/Kg Fuel)
Rice Husk	1.49
Bituminous Coal	2.46
Natural Gas	1.93

5.6. Power Saving Issue

In this work, the performance comparison among existing and proposed sleep mode algorithms has been evaluated through the assumptions described in Table 7. According to the 3GPP TS 23.203 technical specifications, the permissible delay for non-real-time applications is 107 ms, though for specifically IoT applications this is more tolerable. By using the suggested IoT resource schedule algorithm, the proposed model produced greater power saving with a permitted delay, as seen in Figures 26 and 27. Figure 26 demonstrates the proportion of consumption over packet arrival rates. The proposed method consumes less amount of energy than the existing method. In the existing method, if the number of short-cycle is 1 or 2 with a low packet arrival rate, the simulation shows a better result in terms of power consumption than the proposed one. But it is a very small region and if we assume the delay limit is 107 ms, it will be not acceptable because, from Figure 28, we can see that it crosses the delay limit. Therefore, the downlink latency (delay) and the power-saving speed are mutually acceptable. From assumption 2, the results are illustrated in Figures 28 and 29. Here, the percentage of power consumption is greatly improved using the proposed method for a long-range packet arrival rate. For N = 1, 2, or 3, existing methods perform slightly better, as illustrated in Figure 28. However, concerning packet delay, as illustrated in Figure 29, this region is unacceptable. Therefore, the proposed

method is the best choice. From the above analysis, it can be concluded that the proposed method outperforms existing models for NRT applications.

Table 7. Simulation assumptions for sleep mode algorithm.

Parameter	Assumption 1	Assumption 2
τ_S (Short cycle timer length)	20 ms	10 ms
τ_L (Long cycle timer length)	320 ms	640 ms
τ_{st} (Step size timer)	20 ms	20 ms
τ_i (Inactivity timer)	10 ms	10 ms
χ (Packet arrival rate)	0.05 to 0.5 packets/ms	
μ (Service rate)	100 packets/ms	
N (No of short cycles)	1 to 16	
P_{Data} (Power consumption during ON period)	500 mW	
$P_{Inactive}$ (Power consumption during inactivity timer)	255 mW	
P_{OFF} (Power consumption during DRX period)	11 mW	

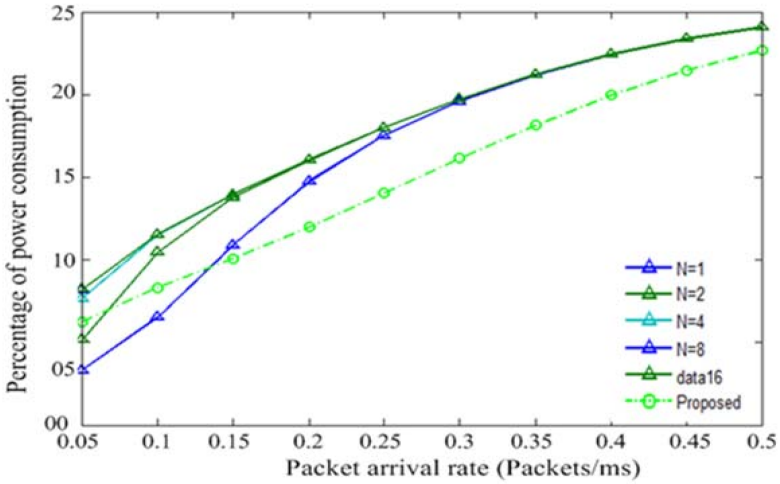

Figure 26. Percentage of power consumption vs. packet arrival rate (Assumption 1).

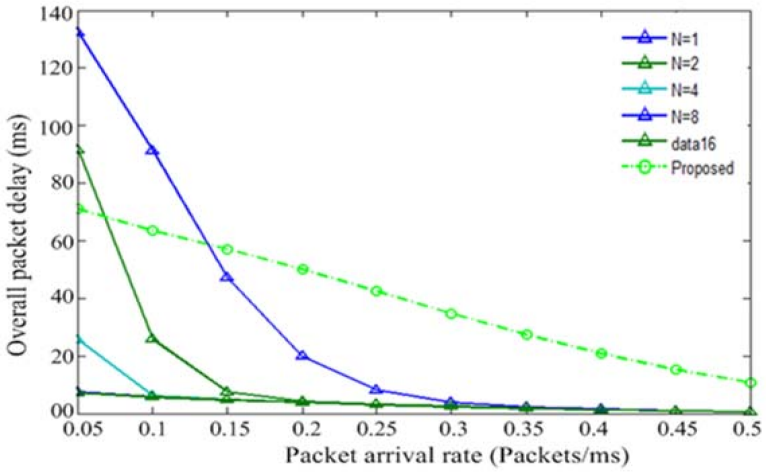

Figure 27. Overall packet delay vs. packet arrival rate (Assumption 1).

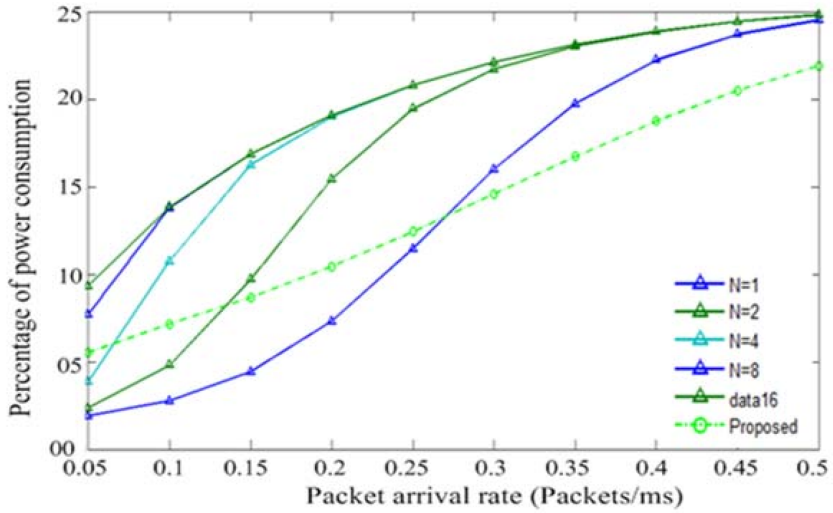

Figure 28. Percentage of power consumption v.s packet arrival rate (Assumption 2).

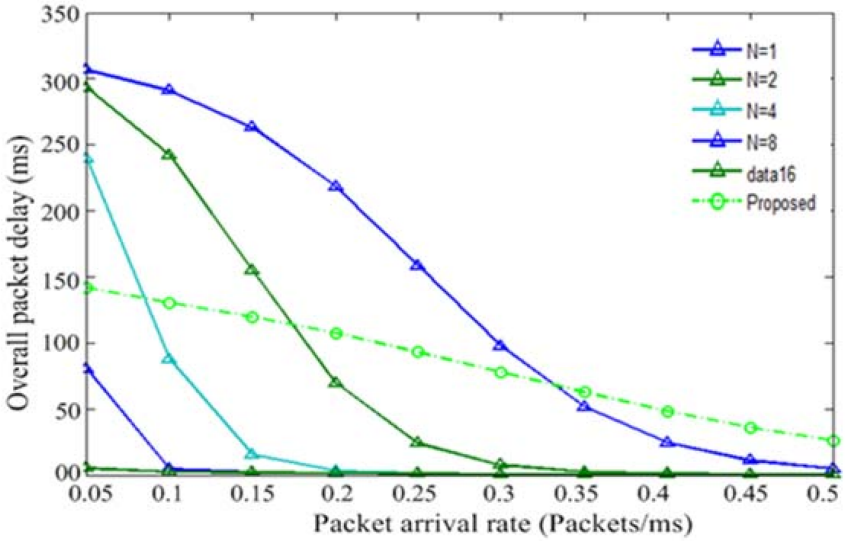

Figure 29. Overall packet delay vs. packet arrival rate (Assumption 2).

5.7. Feasibility Comparison

In order to ensure the effectiveness of the proposed approach, we compared it to some key approaches from the literature. The findings are summarized in Table 8.

From our literature review leading to the above comparison analysis, we noticed that most studies have focused on the key obstacles of establishing a green cellular network that included solar PV and wind turbines as well as a backup system. Furthermore, many of them did not analyze the system for heterogeneous networks. To the best of our knowledge, we are the first to develop a techno-economic and energy efficiency analysis integrating solar PV/BG system with electrical grid system for heterogeneous networks, in addition to the proposed sleep algorithm for IoT applications. Additionally, the suggested system was found to have only have a net present cost of about USD 21,445 and an energy-generating cost of USD 0.379/kWh for the macro-base station. Furthermore, a steady decline in per-unit energy generation cost has been found in response to higher system bandwidth, resulting in lower carbon footprints.

Table 8. A comparison of our work with some published work.

Reference	Software Used	Optimal Size	Brief Summary of the Proposed Technique
[57]	HOMER	8.5 kW PV, 1 kW WT, and N_{batt} = 64.	√ Proposed a solar PV and hybrid solar PV/WT system. √ NPC of USD 30,975, excess energy of 4132 kWh/Yr. √ No GHG.
[58]	HOMER	10 kW PV, 5.5 kW DG, and N_{batt} = 64.	√ Proposed a hybrid solar PV/DG system. √ NPC of USD 69,811, energy cost of USD 0.409/kWh. √ Emits GHG.
[59]	HOMER	2 kW PV, 3 kW WT, and 2 kW FC	√ Proposed a hybrid solar PV/WT and solar PV/WT/FC system. √ NPCs of USD 75,515, excess energy of 3926 kWh/Yr. √ No GHG.
[60]	HOMER	5 kW PV, 1 kW WT, N_{batt} = 16, and 3 kW DG	√ Proposed a hybrid solar PV/WT/DG system. √ Energy cost of USD 0.839/kWh, excess energy of 3792.9 kWh/Yr √ Emits GHG.
[61]	HOMER	2 kW PV, 1 kW WT, N_{batt} = 3, and 1 kW Grid	√ Proposed a hybrid solar PV/WT/Grid system √ NPC of USD 9459, energy cost of USD 0.133/kWh. √ No GHG.
[25]	HOMER MATLAB	2 kW PV, 1 kW WT, and N_{batt} = 32	√ Proposed a hybrid solar PV/WT system. √ NPCs of USD 23,903, excess energy of 863 kWh/Yr. √ No GHG.
[23]	HOMER MATLAB	3.5 kW PV, 1 kW BG, and N_{batt} = 64	√ Proposed a hybrid solar PV/BG system for macro BS. √ NPCs of USD 40,624, energy cost of 0.723 USD/kWh, excess energy of 2094 kWh/Yr. √ Emits GHG.
[Approach proposed in this paper]	HOMER MATLAB	3 kW PV, 1 kW BG, and N_{batt} = 32	√ Proposed a hybrid solar PV/BG/Grid system for HetNet. √ NPCs of USD 21,445, energy cost of USD 0.379/kWh, GHG saving around 2012 Kg/Yr. √ Save GHG by sharing the energy to the grid.

6. Conclusions

This paper proposed a hybrid solar PV/BG-powered heterogeneous cellular network in conjunction with sufficient energy storage devices. Various key performance parameters, including optimal sizing, per unit energy generation cost, harvested energy, shared energy, energy efficiency, and carbon footprints, were evaluated to ensure the viability of the proposed system. To determine the best criteria, extensive simulations were carried out under diverse network circumstances using HOMER optimization software. Simulation results show that locally available renewable energy sources are adequate to supply the heterogeneous network without external support. By ensuring minimal net present cost and per unit capital cost, the proposed system offers sustainable and reliable green mobile communication throughout the year. Moreover, the suggested system would drastically lower carbon footprints, thus resulting in better ecological sustainability compared to conventional power supply options. In addition, appropriate energy storage devices and energy selling mechanisms to the grid improve the reliability of the system by preserving the zero-percent energy shortage/outage. Under a 10MHz macro-configuration, the hybrid system produces 9902 kWh of total energy (66% from solar PV and 34% from BG) and 667 kWh of surplus energy. The numerical results also reveal that the green energy

sharing policy attained energy sharing, yielding up to 3172 kWh and GHG saving around 2012 Kg per year. Additionally, if the hybrid supply system fails to meet the BS energy requirement, the energy storage device can feed the macro- and micro-BSs for 57 h and 255 h, respectively. Moreover, via the effective use of renewable energy, the throughput, and energy efficiency analysis ensures a satisfactory level of wireless performance and data demand. In comparison with the previous approaches, the suggested resource planning algorithm for NRT applications saved a significant amount of electricity.

Author Contributions: Conceptualization, M.S.H., K.Z.I. and A.G.A.; methodology, A.G.A. and M.S.; software, M.S.H. and K.Z.I.; validation, M.S.H., M.S. and M.R.I.; formal analysis, M.S.H. and A.G.A.; investigation, A.G.A. and M.R.I.; resources, M.R.I. and A.F.; data curation, M.S. and A.G.A.; writing—original draft preparation, M.S.H. and A.G.A.; writing—review and editing, K.Z.I., A.F. and M.R.I.; visualization, M.R.I. and A.F.; supervision, M.R.I. and A.F.; project administration, M.S.H. and M.R.I.; funding acquisition, M.R.I. and A.F. All authors have read and agreed to the published version of the manuscript.

Funding: The authors extend their appreciation to the Deputyship for Research & Innovation, Ministry of Education in Saudi Arabia for funding this research work through project number 375213500.

Conflicts of Interest: The authors declare no conflict of interest.

Nomenclature

Summary of the notations and symbols.

Notations/Symbols	Meaning
BG	Biomass generator
BS	Base station
BW	Bandwidth
COE	Cost of energy
DG	Diesel generator
DRX	Discontinuous reception
EE	Energy efficiency
GHG	Greenhouse gas
HetNet	Heterogeneous network
IoT	Internet of Things
NPC	Net present cost
NRT	Non-real-time
PV	Photovoltaic
QoS	Quality of service
WT	Wind turbine
N_{batt}	Number of batteries
χ	Traffic rate

References

1. Jiang, W.; Han, B.; Habibi, M.A.; Schotten, H.D. The Road Towards 6G: A Comprehensive Survey. *IEEE Open J. Commun. Soc.* **2021**, *2*, 334–366. [CrossRef]
2. Han, D.; Li, S.; Peng, Y.; Chen, Z. Energy Sharing-Based Energy and User Joint Allocation Method in Heterogeneous Network. *IEEE Access* **2020**, *8*, 37077–37086. [CrossRef]
3. Ericsson 2020 Mobility Report Summary. Available online: https://www.microwavejournal.com/blogs/9-pat-hindle-mwj-editor/post/34139-ericsson-2020-mobility-report-summary?gclid=Cj0KCQiA15yNBhDTARIsAGnwe0VcFe1y1xFyFJcUPPEMSFFiBVJ1dosg2wE8eONvi7bNS9Gh4kz-HNQaAsj3EALw_wcB (accessed on 20 December 2021).
4. Jiang, Y.; Zou, Y.; Guo, H.; Tsiftsis, T.A.; Bhatnagar, M.R.; de Lamare, R.C.; Yao, Y.-D. Joint Power and Bandwidth Allocation for Energy-Efficient Heterogeneous Cellular Networks. *IEEE Trans. Commun.* **2019**, *67*, 6168–6178. [CrossRef]
5. Li, Y.; Zhang, H.; Wang, J.; Cao, B.; Liu, Q.; Daneshmand, M. Energy-Efficient Deployment and Adaptive Sleeping in Heterogeneous Cellular Networks. *IEEE Access* **2019**, *7*, 35838–35850. [CrossRef]
6. Why China's Mobile Coverage Is Superior to That of the US. Available online: https://www.globaltimes.cn/content/1172513.shtml (accessed on 20 December 2021).
7. Chettri, L.; Bera, R. A Comprehensive Survey on Internet of Things (IoT) Toward 5G Wireless Systems. *IEEE Internet Things J.* **2020**, *7*, 16–32. [CrossRef]

8. Liu, S.; Liu, L.; Yang, H.; Yue, K.; Guo, T. Research on 5G Technology Based on Internet of Things. In Proceedings of the 2020 IEEE 5th Information Technology and Mechatronics Engineering Conference (ITOEC), Chongqing, China, 12–14 June 2020; pp. 1821–1823.
9. Reddy, M.P.; Kumar, A.; Kuchi, K. Joint Control and Shared Channel Scheduling for Downlink in 3GPP Narrowband-IoT. In Proceedings of the 2020 International Conference on COMmunication Systems NETworkS (COMSNETS), Bengaluru, India, 7–11 January 2020; pp. 476–483.
10. Manne, P.R.; Ganji, S.; Kumar, A.; Kuchi, K. Scheduling and Decoding of Downlink Control Channel in 3GPP Narrowband-IoT. *IEEE Access* **2020**, *8*, 175612–175624. [CrossRef]
11. Wu, J.; Zhang, Y.; Zukerman, M.; Yung, E.K.-N. Energy-Efficient Base-Stations Sleep-Mode Techniques in Green Cellular Networks: A Survey. *IEEE Commun. Surv. Tutor.* **2015**, *17*, 803–826. [CrossRef]
12. World's Leading Mobile Operators to Disclose Climate Impacts as Part of New GSMA-Led Climate Action Roadmap. Available online: https://www.gsma.com/newsroom/press-release/worlds-leading-mobile-operators-to-disclose-climate-impacts-as-part-of-new-gsma-led-climate-action-roadmap/ (accessed on 20 December 2021).
13. World Energy Outlook. 2018. Available online: https://www.iea.org/reports/world-energy-outlook-2018 (accessed on 20 December 2021).
14. Jahid, A.; Shams, A.B.; Hossain, M.F. Dynamic Point Selection Comp Enabled Hybrid Powered Green Cellular Networks. *Comput. Electr. Eng.* **2018**, *72*, 1006–1020. [CrossRef]
15. Jahid, A.; Monju, K.H.; Hossain, S.; Hossain, F. Hybrid Power Supply Solutions for Off-Grid Green Wireless Networks. *Int. J. Green Energy* **2019**, *16*, 12–33. [CrossRef]
16. Hossain, M.S.; Jahid, A.; Rahman, M.F. Dynamic Load Management Framework for off-Grid Base Stations With Hybrid Power Supply. In Proceedings of the 4th International Conference on Electrical Engineering and Information & Communication Technology (iCEEiCT), Dhaka, Bangladesh, 13–15 September 2018; pp. 336–341. [CrossRef]
17. Jahid, A.; Hossain, M.S.; Monju, M.K.H.; Rahman, M.F.; Hossain, M.F. Techno-Economic and Energy Efficiency Analysis of Optimal Power Supply Solutions for Green Cellular Base Stations. *IEEE Access* **2020**, *8*, 43776–43795. [CrossRef]
18. 3GPP TS 43.013, Discontinuous Reception (DRX) in the GSM System. Status: Under Change Control, Rel. 4. 2016. Available online: https://portal.3gpp.org/desktopmodules/Specifications/SpecificationDetails.aspx?specificationId=2661 (accessed on 20 December 2021).
19. Alsharif, M.H. Techno-Economic Evaluation of a Stand-Alone Power System Based on Solar Power/Batteries for Global System for Mobile Communications Base Stations. *Energies* **2017**, *10*, 392. [CrossRef]
20. Chamola, V.; Sikdar, B. Solar Powered Cellular Base Stations: Current Scenario, Issues and Proposed Solutions. *IEEE Commun. Mag.* **2016**, *54*, 108–114. [CrossRef]
21. Alsharif, M.H.; Nordin, R.; Ismail, M. Energy Optimisation of Hybrid Off-Grid System for Remote Telecommunication Base Station Deployment in Malaysia. *EURASIP J. Wirel. Commun. Netw.* **2015**, *2015*, 64. [CrossRef]
22. Han, T.; Ansari, N. On Optimizing Green Energy Utilization for Cellular Networks with Hybrid Energy Supplies. *IEEE Trans. Wirel. Commun.* **2013**, *12*, 3872–3882. [CrossRef]
23. Hossain, M.S.; Rahman, M.F. Hybrid Solar PV/Biomass Powered Energy Efficient Remote Cellular Base Stations. *Int. J. Renew. Energy Res.* **2020**, *10*, 329–342.
24. Hossain, M.S.; Islam, K.Z.; Jahid, A.; Rahman, K.M.; Ahmed, S.; Alsharif, M.H. Renewable Energy-Aware Sustainable Cellular Networks with Load Balancing And Energy-Sharing Technique. *Sustainability* **2020**, *12*, 9340. [CrossRef]
25. Jahid, A.; Monju, M.K.H.; Hossain, M.E.; Hossain, M.F. Renewable Energy Assisted Cost Aware Sustainable Off-Grid Base Stations with Energy Cooperation. *IEEE Access* **2018**, *6*, 60900–60920. [CrossRef]
26. Hossain, M.S.; Jahid, A.; Islam, K.Z.; Rahman, M.F. Solar PV and Biomass Resources-Based Sustainable Energy Supply for Off-Grid Cellular Base Stations. *IEEE Access* **2020**, *8*, 53817–53840. [CrossRef]
27. Mohaghegh, M.R.; Heidari, M.; Tasnim, S.; Dutta, A.; Mahmud, S. Latest Advances on Hybrid Solar–Biomass Power Plants. *Energy Sources Part A Recovery Util. Environ. Eff.* **2021**, *1*, 1–24. [CrossRef]
28. Aziz, A.S.; Tajuddin, M.F.N.B.; bin Adzman, M.R. Feasibility Analysis of PV/Wind/Battery Hybrid Power Generation: A Case Study. *Int. J. Renew. Energy Res.* **2018**, *8*, 661–671.
29. Farooq, M.J.; Ghazzai, H.; Kadri, A.; Elsawy, H.; Alouini, M.S. A Hybrid Energy Sharing Framework for Green Cellular Networks. *IEEE Trans. Commun.* **2017**, *65*, 918–934. [CrossRef]
30. Al-Ghussain, L.; Samu, R.; Taylan, O.; Fahrioglu, M. Sizing Renewable Energy Systems with Energy Storage Systems in Microgrids for Maximum Cost-Efficient Utilization of Renewable Energy Resources. *Sustain. Cities Soc.* **2020**, *55*, 102059. [CrossRef]
31. E-Plus, Nokia Siemens Networks Build Germany First Offgrid Base Station. Available online: http://www.nokiasiemensnetworks.com (accessed on 20 December 2021).
32. Chia, Y.-K.; Sun, S.; Zhang, R. Energy Cooperation in Cellular Networks with Renewable Powered Base Stations. *IEEE Trans. Wirel. Commun.* **2014**, *13*, 6996–7010. [CrossRef]
33. Jahid, A.; Ahmad, A.S.; Hossain, M.F. Energy Efficient BS Cooperation in DPS Comp Based Cellular Networks with Hybrid Power Supply. In Proceedings of the 2016 19th International Conference on Computer and Information Technology (ICCIT), Dhaka, Bangladesh, 18–20 December 2016; pp. 93–98.

34. Ugwoke, B.; Corgnati, S.P.; Leone, P.; Borchiellini, R.; Pearce, J.M. Low Emissions Analysis Platform Model for Renewable Energy: Community-Scale Case Studies in Nigeria. *Sustain. Cities Soc.* **2021**, *67*, 102750. [CrossRef]
35. Awad, H.; Gül, M. Optimisation of Community Shared Solar Application in Energy Efficient Communities. *Sustain. Cities Soc.* **2018**, *43*, 221–237. [CrossRef]
36. Ye, Q.; Rong, B.; Chen, Y.; Al-Shalash, M.; Caramanis, C.; Andrews, J.G. User Association for Load Balancing in Heterogeneous Cellular Networks. *IEEE Trans. Wirel. Commun.* **2013**, *12*, 2706–2716. [CrossRef]
37. Kim, D.H.; Kim, H.S.; Lee, D.W. Packet Scheduling Algorithm For NRT Service in Wireless System Supporting Integrated Services of RT and NRT Applications. In Proceedings of the 2007 International Symposium on Communications and Information Technologies, Sydney, NSW, Australia, 17–19 October 2007; pp. 500–504.
38. Lin, Y.; Yue, G. Channel-Adapted and Buffer-Aware Packet Scheduling in LTE Wireless Communication System. In Proceedings of the 2008 4th International Conference on Wireless Communications, Networking and Mobile Computing, Dalian, China, 12–14 October 2008; pp. 1–4.
39. Li, Q.; Hu, R.Q.; Qian, Y.; Wu, G. A Proportional Fair Radio Resource Allocation for Heterogeneous Cellular Networks with Relays. In Proceedings of the 2012 IEEE Global Communications Conference (GLOBECOM), Anaheim, CA, USA, 3–7 December 2012; pp. 5457–5463.
40. Wang, H.-C.; Tseng, C.-C.; Chen, G.-Y.; Kuo, F.-C.; Ting, K.-C. Power Saving by LTE DRX Mechanism Using a Mixture of Short and Long Cycles. In Proceedings of the 2013 IEEE International Conference of IEEE Region 10 (TENCON 2013), Xi'an, China, 22–25 October 2013; pp. 1–6.
41. Zhou, L.; Xu, H.; Tian, H.; Gao, Y.; Du, L.; Chen, L. Performance Analysis of Power Saving Mechanism with Adjustable DRX Cycles in 3GPP LTE. In Proceedings of the 2008 IEEE 68th Vehicular Technology Conference, Calgary, AB, Canada, 21–24 September 2008; pp. 1–5.
42. Fowler, S.; Bhamber, R.S.; Mellouk, A. Analysis of Adjustable and Fixed DRX Mechanism for Power Saving in LTE/LTE-Advanced. In Proceedings of the 2012 IEEE International Conference on Communications (ICC), Ottawa, ON, Canada, 10–15 June 2012; pp. 1964–1969.
43. Liu, Y.; Huynh, M.; Mangla, A.; Ghosal, D. Performance Analysis of Adjustable Discontinuous Reception (DRX) Mechanism in LTE Network. In Proceedings of the 2014 23rd Wireless and Optical Communication Conference (WOCC), Newark, NJ, USA, 9–10 May 2014; pp. 1–6.
44. Karthik, R.M.; Chakrapani, A. Practical Algorithm for Power Efficient DRX Configuration in Next Generation Mobiles. In Proceedings of the 2013 Proceedings IEEE INFOCOM, Turin, Italy, 14–19 April 2013; pp. 1106–1114.
45. Hossain, M.S.; Alharbi, A.G.; Islam, K.Z.; Islam, M.R. Techno-Economic Analysis of the Hybrid Solar PV/H/Fuel Cell Based Supply Scheme for Green Mobile Communication. *Sustainability* **2021**, *13*, 12508. [CrossRef]
46. Mondal, M.A.H.; Islam, A.K.M.S. Potential and Viability of Grid-Connected Solar PV System in Bangladesh. *Renew. Energy* **2011**, *36*, 1869–1874. [CrossRef]
47. Ahiduzzaman, M.; Islam, A.K.M.S. Energy Utilization and Environmental Aspects of Rice Processing Industries in Bangladesh. *Energies* **2009**, *2*, 134–149. [CrossRef]
48. Huda, A.S.N.; Mekhilef, S.; Ahsan, A. Biomass Energy in Bangladesh: Current Status and Prospects. *Renew. Sustain. Energy Rev.* **2014**, *30*, 504–517. [CrossRef]
49. Islam, M.S.; Akhter, R.; Rahman, M.A. A Thorough Investigation on Hybrid Application of Biomass Gasifier and PV Resources To Meet Energy Needs for a Northern Rural Off-Grid Region of Bangladesh: A potential solution to replicate in rural off-grid areas or not? *Energy* **2018**, *145*, 338–355. [CrossRef]
50. Halder, P.K.; Paul, N.; Beg, M.R.A. Assessment of Biomass Energy Resources and Related Technologies Practice in Bangladesh. *Renew. Sustain. Energy Rev.* **2014**, *39*, 444–460. [CrossRef]
51. Alsharif, M.H.; Kim, J. Hybrid Off-Grid SPV/WTG Power System for Remote Cellular Base Stations Towards Green and Sustainable Cellular Networks in South Korea. *Energies* **2017**, *10*, 9. [CrossRef]
52. Chauhan, A.; Saini, R.P. A review on Integrated Renewable Energy System Based Power Generation for Stand-Alone Applications: Configurations, Storage Options, Sizing Methodologies and Control. *Renew. Sustain. Energy Rev.* **2014**, *38*, 99–120. [CrossRef]
53. Holtkamp, H.; Auer, G.; Giannini, V.; Haas, H. A Parameterized Base Station Power Model. *IEEE Commun. Lett.* **2013**, *17*, 2033–2035. [CrossRef]
54. Auer, G.; Giannini, V.; Desset, C.; Godor, I.; Skillermark, P.; Olsson, M.; Imran, M.A.; Sabella, D.; Gonzalez, M.J.; Blume, O.; et al. How Much Energy is Needed to Run a Wireless Network? *IEEE Wirel. Commun.* **2011**, *18*, 40–49. [CrossRef]
55. Jin, S.; Qiao, D. Numerical Analysis of the Power Saving in 3GPP LTE Advanced Wireless Networks. *IEEE Trans. Veh. Technol.* **2012**, *61*, 1779–1785. [CrossRef]
56. Alsharif, M.H.; Kannadasan, R.; Jahid, A.; Albreem, M.A.; Nebhen, J.; Choi, B.J. Long-Term Techno-Economic Analysis of Sustainable and Zero Grid Cellular Base Station. *IEEE Access* **2021**, *9*, 54159–54172. [CrossRef]
57. Alsharif, M.H.; Kim, J.; Kim, J.H. Energy optimization Strategies for Eco-Friendly Cellular Base Stations. *Energies* **2018**, *11*, 1500. [CrossRef]
58. Olatomiwa, L.; Mekhilef, S.; Huda, A.S.N.; Sanusi, K. Techno-Economic Analysis of Hybrid PV—Diesel-Battery and PV—Wind-Diesel-Battery Power Systems for Mobile BTS: The Way Forward for Rural Development. *Energy Sci. Eng.* **2015**, *3*, 271–285. [CrossRef]

59. Amutha, W.M.; Rajini, V. Techno-Economic Evaluation of Various Hybrid Power Systems for Rural Telecom. *Renew. Sustain. Energy Rev.* **2015**, *43*, 553–561. [CrossRef]
60. Asif, R.; Khanzada, F. Cellular Base Station Powered by Hybrid Energy Options. *Int. J. Comput. Appl.* **2015**, *115*, 35–39. [CrossRef]
61. Alsharif, M.H.; Nordin, R.; Ismail, M. Green Wireless Network Optimisation Strategies Within Smart Grid Environments for Long Term Evolution (LTE) Cellular Networks in Malaysia. *Renew. Energy* **2016**, *85*, 157–170. [CrossRef]